IEEE Photonics Journal
An IEEE Photonics Society Publication

Open Access

A Simplified Radio-Over-Fiber System for Over 100-km Long-Reach n-QAM Transmission

Volume 12, Number 3, June 2020

Run-Kai Shiu
You-Wei Chen
Peng-Chun Peng
Shang-Jen Su
Guan-Ming Shao
Justin Chiu
Jyun-Wei Li
Gee-Kung Chang, *Fellow, IEEE*

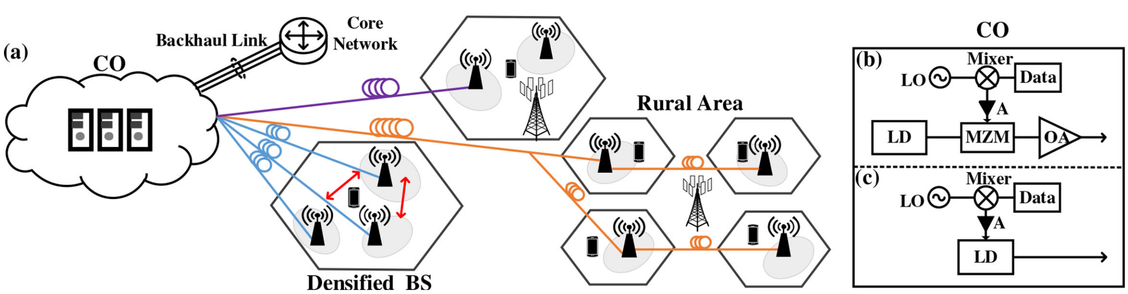

DOI: 10.1109/JPHOT.2020.2993180

IEEE photonics SOCIETY
IEEE

A Simplified Radio-Over-Fiber System for Over 100-km Long-Reach n-QAM Transmission

Run-Kai Shiu,[1,2] You-Wei Chen,[2] Peng-Chun Peng,[1] Shang-Jen Su,[2] Guan-Ming Shao,[1] Justin Chiu,[1] Jyun-Wei Li,[1] and Gee-Kung Chang,[2] *Fellow, IEEE*

[1]Department of Electro-Optical Engineering, National Taipei University of Technology, Taipei 10608, Taiwan
[2]School of Electrical and Computer Engineering, Georgia Institute of Technology, Atlanta 30308 USA

DOI:10.1109/JPHOT.2020.2993180

Manuscript received April 27, 2020; accepted May 3, 2020. Date of publication May 7, 2020; date of current version May 26, 2020. This work was supported by the Ministry of Science and Technology, Taiwan, under Grants MOST 108-2221-E-027 -040 -MY2 and MOST 108-2917-I-027 -001. Corresponding author: Peng-Chun Peng (e-mail: pcpeng@ntut.edu.tw).

Abstract: A simplified and cost-effective architecture is proposed and experimentally demonstrated with a millimeter wave (MMW) signal over fiber and free-space wireless transmission. The distributed feedback (DFB) laser is operated in optimized settings after measuring its characteristics and thus the 6 Gbps 64–quadrature amplitude modulation (64-QAM) signal can be successfully transmitted after 20- and 50-km fiber and 1-meter wireless transmission with EVM of 5.98% and 6.87%, respectively. Moreover, the EVM of 10.8% over 100-km long reach is also achieved with the 32-QAM modulation format and data rate of 5 Gbps. The experimental results show that the proposed direct modulation scheme can satisfy applications in metro and rural areas.

Index Terms: Radio-over-fiber system, fiber-wireless access network, direct modulation.

1. Introduction

Optical communication systems have developed rapidly in diverse application scenarios [1]–[8]. Radio-over-fiber (RoF) technique allows the up-conversion devices and baseband signal processors to be removed from the base station (BS) and centralized in the central office (CO) through the optical network as shown in Fig. 1(a), and thus it can easily extend the millimeter wave signal (MMW) signal coverage through fiber [9]–[15]. With the help of RoF technology, the densified BS and long-distance transmission can be achieved for the radio access network (RAN) architecture. As shown in Fig. 1(b), a continuous laser and an external modulator are commonly used in the RoF system since the external modulator usually has higher operation frequency and less chirping as compared with the directly modulated laser (DML) [16], [17]. In the external modulator based scheme, some optical single sideband (OSSB) modulation techniques such as using dual-parallel Mach-Zehnder modulator (DP-MZM) or dual-drive MZM have been proposed to mitigate the RF fading effect [18], [19]. However, MZM typically suffers from the DC drift problem and the external modulator also has high insertion loss, which limits the power budget of the system. Therefore, to develop a cost-effective and simple transmitter design for the RAN architecture, DML is a promising

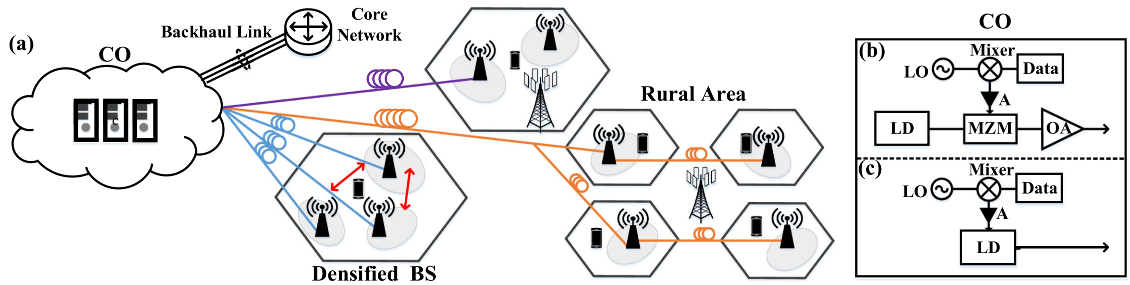

Fig. 1. (a) Schematic diagram of the RAN architecture. (b) External modulation based transmitter. (c) Direct modulation based transmitter. CO: central office, LO: local oscillator, A: amplifier, LD: laser diode, MZM: Mach-Zehnder modulator, OA: optical amplifier, and BS: base station.

alternative due to its advantages, such as high energy efficiency and linear characteristic. However, the commercial DML usually has a limited operation bandwidth of 10 GHz. In a DML-based RoF system as shown in Fig. 1(c), it requires an optical multitones generation for obtaining higher RF frequency signals and applies the narrow-band optical filter to select the specific wavelengths. The desired MMW signal can be generated after optical filtering and then heterodyne beating via a photo detector (PD). The stability and the flatness of the generated multitones in the conventional DML-based RoF system would restrict its feasibility. Thus, a simplified DML-based RoF system is desired. Recently, only a limited number of works using DML with high operation bandwidth to carry the MMW signal have been reported. A distributed feedback (DFB) laser is modulated by a 1 Gbps quadrature phase shift keying (QPSK) signal at the carrier frequency of 24 GHz over 50-km fiber transmission [20]. However, the measured error vector magnitude (EVM) performance is insufficient and it can only support QPSK modulation format with low spectral efficiency. A vertical-cavity surface-emitting laser (VCSEL) is directly modulated by a 32-quadrature amplitude modulation (32-QAM) signal at 28 GHz [21]. The EVM of 8.02% was achieved after 2-km SSMF transmission. The short fiber-link and the lack of wireless transmission limit the application scenario. An RoF system with free space transmission using a DML to carry a 24-GHz 64-QAM signal is proposed [22]. Good EVM performance of 4.7% was achieved after fiber and free-space optics transmission. However, the fiber length is only 1-km and the signal baud rate is only 100MHz which limits the system flexibility and application scope.

In this paper, a 24-GHz MMW-RoF system based on a direct modulation scheme with 20-/50-/100-km fiber-links and 1-meter wireless transmission is proposed. The DFB laser utilized in the proposed scheme can support up to 25 GHz frequency operation and its frequency responses versus different injection currents and the stability of generated optical tones have been investigated in [23]. Therefore, the 24-GHz signal can be directly generated via the DFB laser without any optical pre-operation. By optimizing the operation settings of the DFB laser, 6 Gbps 64-QAM signals are successfully transmitted over 20- and 50-km fibers. For 100-km fiber transmission, the OSSB signal is generated by applying the passive component, interleaver (IL), to remove the left optical sideband of the 24-GHz signal. By mitigating the effect of RF fading, 5 Gbps 32-QAM signal is achieved after 100-km fiber link and 1-meter wireless transmission. The experimental results reveal that the 24-GHz MMW signal can be supported via a direct modulation RoF system with different transmission distances for metro and rural areas with simplified and cost-effective architecture.

2. Experimental setup

Fig. 2 depicts the experimental setup of the proposed direct modulation MMW-RoF system for different transmission distances. The DFB laser is employed as the light source and driven by a commercial current controller and a temperature controller to stabilize the output power and wavelength. A 1 Gbaud 24-GHz signal is generated from the arbitrary waveform generator (AWG,

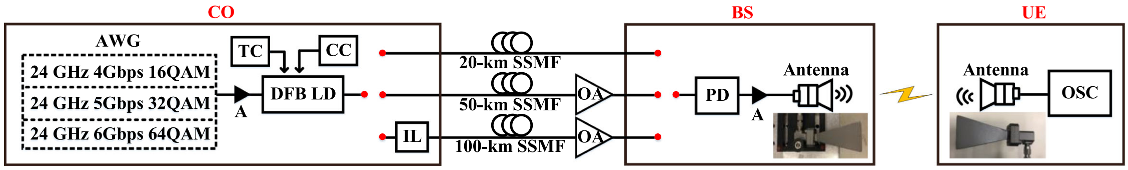

Fig. 2. Experimental setup of the proposed direct modulation system. DFB LD: distributed feedback laser diode, TC: temperature controller, CC: current controller, SSMF: standard single mode fiber, IL: interleaver, PD: photodetector, and OSC: oscilloscope.

Keysight M8195A) and boosted via an 18dB-gain amplifier before launched into the DFB. For 20-km fiber transmission, no optical amplifier is required since the output optical power of the DFB laser is already high enough for signal delivery. For 50- and 100-km fiber transmissions, an EDFA is employed after the fiber transmission to increase the received optical power (ROP) for compensating the fiber loss. In our proposed scheme, no additional filter is employed for 20- and 50-km link. However, due to the nature of double sideband intensity modulation, chromatic dispersion induced RF power fading is severe after 100-km fiber transmission. Thus, an IL with 100-GHz wavelength spacing is employed to remove one of the optical sidebands to mitigate the effect of RF fading. After standard single-mode fiber (SSMF) transmission, a commercial photodetector (PD) is used to directly up-convert the desired data to the MMW frequency, i.e., 24 GHz. A 30-dB gain amplifier is applied to boost the electrical signal before the 19-dBi gain K-band antenna. Up to 5-meter wireless transmission is demonstrated in the 25-km fiber link and the wireless transmission distance can be effectively extended when additional large gain amplifiers are employed [24]. In the user equipment (UE) side, the 24-GHz signal is received by another paired K-band antenna and evaluated by the built-in Vector Signal Analysis (VSA) software on the oscilloscope (OCS, Keysight DSOZ254A) in terms of its EVM, signal-to-noise ratio (SNR), and constellation diagrams.

3. Experimental Results

3.1 Measurement of the DFB laser

To demonstrate the linearity characteristic of the employed DFB laser, we measured the I-P curve by changing the driving current of the DFB laser from 0 to 150 mA with an increment of 5 mA as shown in Fig. 3(a). The threshold current of the DFB laser is about 25 mA and it exhibits high linearity within the testing range of driving current from 25 to 150 mA. Fig. 3(b) shows the optical spectra with different driving current settings of the DFB laser. With higher driving current, the wavelength is red-shifted and the sidemode suppression ratio of the DFB laser is also increased, which can achieve $>$50 dB at the driving current setting of 150 mA. Fig. 3(c) shows the optical spectra of the DFB laser driven by 130 mA before and after modulated by a 24-GHz 16-QAM signal. The wavelength spacing between the optical carrier and the first-order optical sidebands is 24 GHz. Since it is a direct intensity modulation, both the desired 24-GHz signal and the unwanted frequency doubling term at 48 GHz appear simultaneously after heterodyne detection. While the unwanted 48 GHz signal can be easily removed by the employed antenna with a passband of 18-40 GHz and thus it would not saturate the receiving front-end.

As illustrated in Fig. 3(c), the double optical sideband signals will induce RF power fading caused by chromatic dispersion after fiber transmission. Moreover, in theoretical, it becomes more severe in the direct detection scheme when the transmission distance is longer. Therefore, to investigate the impairment of RF fading in the proposed system, a multi-tone signal starting from 0 to 25 GHz with 200 carriers and 50 MHz frequency spacing is launched into the DFB laser and its electrical spectra after different fiber transmission distances with the fixed ROP of 3 dBm at the receiver side are measured. The electrical spectra after 20-, 50-, 75- and 100-km SSMF transmission are shown in Fig. 4(a)-(d). The number of frequency notches is increasing as the transmission distance is

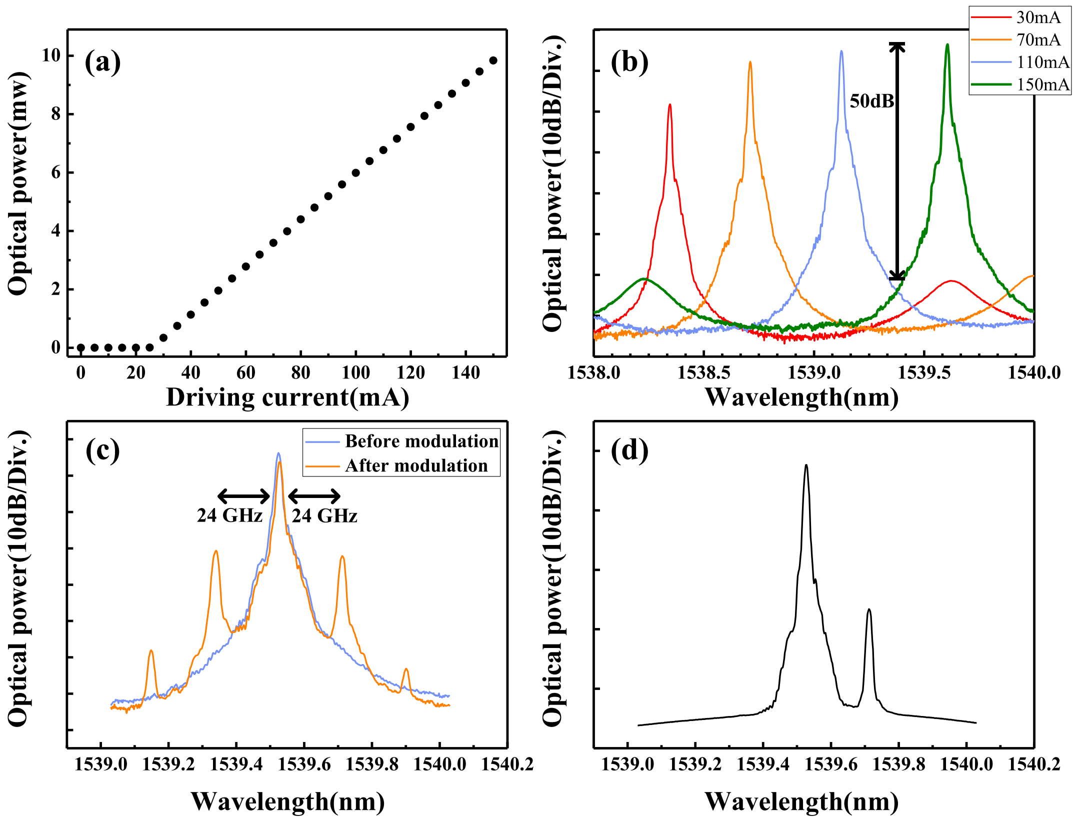

Fig. 3. (a) Measured optical output power versus different driving currents. Measured optical spectra of the DFB laser (b) driven by different current settings at the transmitter output, (c) before and after 24-GHz signal modulation, and (d) after applying IL for 100-km transmission.

increasing. As one can note that 24-GHz signal can be survived after all the transmission distances except the 100-km transmission case. As we apply a 1Gbaud 24-GHz signal for 100-km fiber transmission, the frequency notch causes significant power degradation as shown in Fig. 4(e). To address this issue, we employ an IL to remove the left optical sideband of the modulated signal as shown in Fig. 3(d) to generate the OSSB signal. Fig. 4(f) shows the frequency notch at 24 GHz is conquered with the help of OSSB generation.

3.2 Performance of Transmission

3.2.1 20-km Transmission: For 20-km fiber transmission, we focus on developing a simple and cost-effective scheme to facilitate the densified BS deployment without any optical filter and amplifier. The EVM performance versus driving voltages of a 1Gbaud 16-QAM signal at 24 GHz after 20-km fiber link and 1-meter wireless transmission is measured under the same ROP of 3 dBm and different driving current settings. The driving voltage denotes the output peak-to-peak voltage (Vpp) from the AWG before the amplification. As shown in Fig. 5(a), for all driving current settings, the lowest EVM can be observed when the driving voltage is 600 mV and the constellation diagrams of driving current at 130 mA is presented. To compare the EVM among different driving current settings, the driving voltage is fixed at 600 mV and the EVM performances with different driving currents from 90 to 150 mA are measured as shown in Fig. 5(b). The results indicate that the best EVM performance is observed when the driving current is 90 mA. This can be understood since the amplitude of the desired RF is fixed via the output voltage. If we further increase the driving current, it would only increase the optical carrier power and the carrier-to-signal power

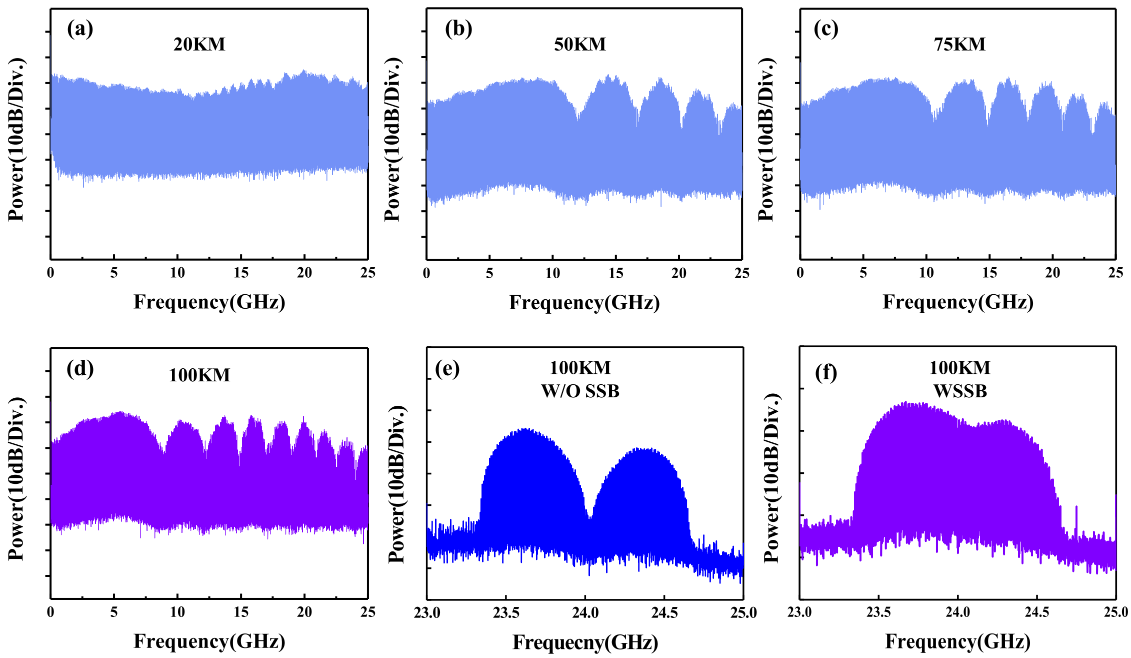

Fig. 4 Measured electrical spectra of the multitone signals after (a) 20-km, (b) 50-km, (c) 75-km, and (d) 100-km fiber transmission. Measured electrical spectra of 24-GHz 16-QAM signal in the 100-km fiber link (e) without SSB and (f) with SSB.

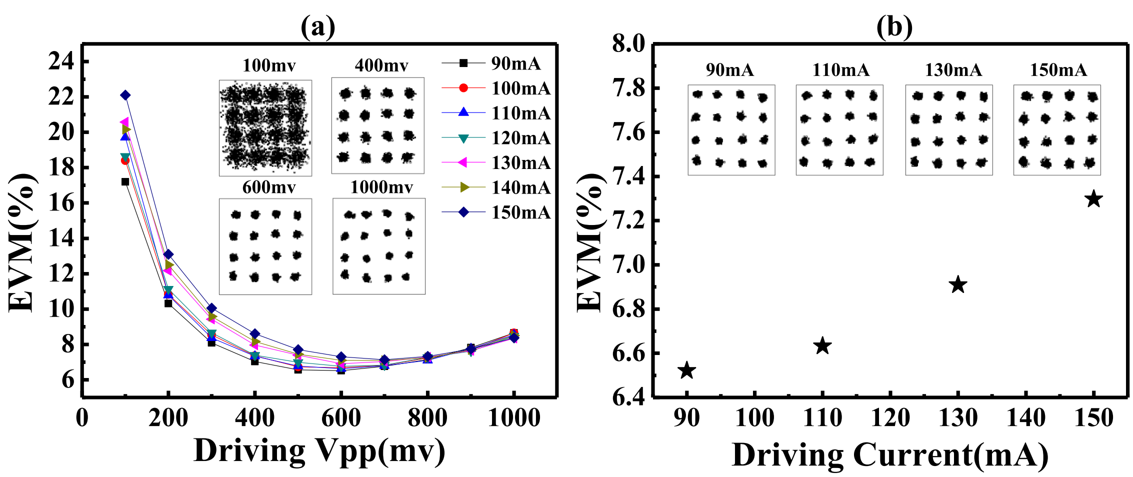

Fig. 5 The EVM and constellation diagrams of the DFB laser driven by (a) different voltages and current settings, and (b) different currents with fixed Vpp of 600 mV.

ratio (CSPR). In a fixed received power system, SNR of the desired signal reduces as the CSPR increases [25]. However, the average output power of the DML is decreased when a lower driving current is applied and it may defeat the purpose of getting rid of the optical amplifier. Thus, there is a trade-off between EVM and optical output power. Although the EVM performance of 90 mA is better than that of 130 mA, the ROP of 130 mA can reach up to 5 dBm at the receiver side, which is 2 dB higher than that of 90 mA. Moreover, the wavelength of the DFB laser driven by 130 mA is 1530.53 nm, which fits well with the employed IL for the single sideband generation. Therefore, under considering the factors described above, the DFB laser is driven by 130 mA with 9.33 dBm output power and directly modulated via a 24-GHz 16-QAM signal at 600 mV in this

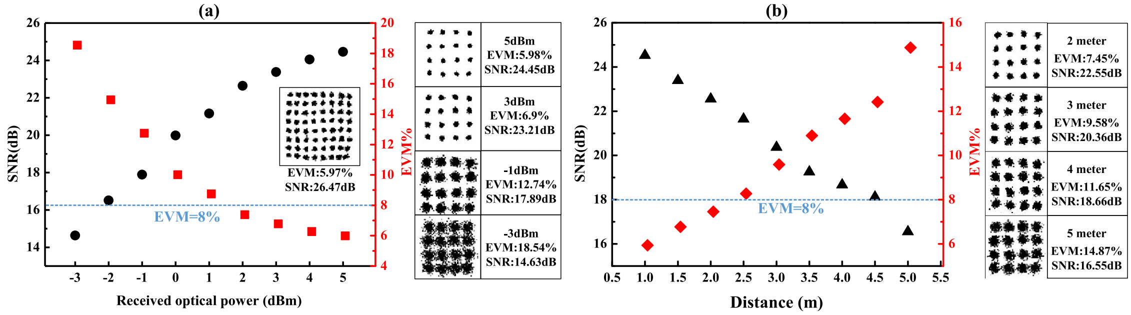

Fig. 6. Measured SNR and EVM with recorded constellation diagrams versus (a) different ROPs, and (b) different wireless transmission distances.

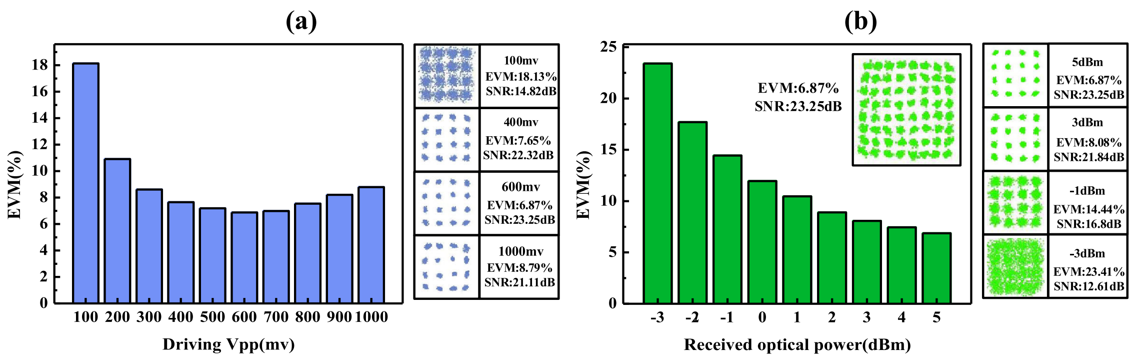

Fig. 7. Measured SNR and EVM with recorded constellation diagrams of 50-km fiber link and 1-meter wireless transmission versus (a) different driving voltages, and (b) different ROPs.

demonstration. Fig. 6(a) shows the SNR, EVM, and the constellation diagrams of the 16-QAM signal versus different ROPs after 1-meter wireless transmission. The SNR of 24.45dB is achieved when the ROP is 5 dBm. The best and the worst EVM are 5.98% and 18.54% with ROP of 5 dBm and -3 dBm, respectively. Since the EVM floor of 8% is achieved, which meets the FEC threshold requirement [26], [27] of 64-QAM signal, we launched the 64-QAM signal into the DFB laser to increase the data rate to 6 Gbps. The corresponding constellation diagram of 64-QAM signal is shown in the inset of Fig. 6(a). The wireless transmission distance for 24-GHz MMW signal is investigated and the EVM performance of 1Gbaud 16-QAM signal over 1-5 meters are measured. The SNR and EVM performances versus different wireless transmission distances are shown in Fig. 6(b). The EVM can reach the FEC threshold of 17% for 16-QAM signal after 5-meter wireless transmission.

3.2.2 50-km Transmission: For the 50-km fiber transmission, an additional EDFA is employed to boost the optical power to compensate the transmission loss. Fig. 7(a) shows the EVM performance of 24-GHz 16-QAM signal versus different driving voltages after 50-km SSMF and 1-meter wireless transmission. Same as the 20-km fiber link, the driving voltage of 600 mV exhibits the best EVM performance. Thus, the 24-GHz 16-QAM signal with 600 mV is sent into the DFB laser to test the EVM performance versus different ROPs as shown in Fig. 7(b). A 24-GHz 64-QAM signal is applied to the DFB laser and the EVM of 6.87% is achieved when the ROP is 5 dBm. Compared to 20-km fiber transmission, the EVM value of 50-km fiber link only increases about 0.9% which is still below the FEC threshold by 1.13%.

3.2.3 100-km Transmission: In order to remove the left optical sideband, an IL is utilized before 100-km fiber transmission. The electrical spectra of 24-GHz 16-QAM signal with and without SSB generation are shown in Fig. 4. Without employing the IL, the 16-QAM signal encounters

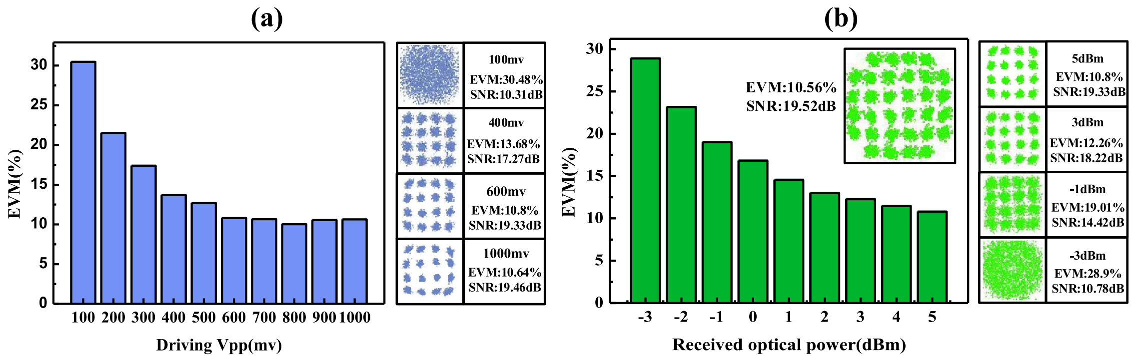

Fig. 8. Measured SNR and EVM with recorded constellation diagrams of 100-km fiber link and 1-meter wireless transmission versus (a) different driving voltages, and (b) different ROPs.

TABLE 1
Comparison of all Three-Transmission Distances

Transmission Distance	Optical Amplifier	Optical Filter	QAM Format	Data Rate	Best EVM
20 km	x	x	64-QAM	6 Gbps	5.98%
50 km	v	x	64-QAM	6 Gbps	6.87%
100 km	v	v	32-QAM	5 Gbps	10.8%

a frequency notch at 24 GHz and experiences a significant degradation, as shown in Fig. 4(e). On the contrary, Fig. 4(f) shows the electrical spectrum of the 16-QAM signal with the help of IL and the RF fading issue can be mediated. The EVM performance for 100-km fiber link and 1-meter wireless transmission versus different driving voltages is shown in Fig. 8(a). The EVM is below the floor of 12% in the range of the driving voltage from 600 mV to 1000 mV. Therefore, the driving voltage is still set to 600 mV considering the lower power consumption and fair comparison of transmission performance among all the experiment settings. Fig. 8(b) shows the EVM performance with varied ROPs; the 32-QAM signal is applied since the EVM performance of 5 dBm ROP is lower than 12%. Table 1 summarizes the transmission performance among 20-/50-/100-km fiber links. 6 Gbps data rate is achieved in 20- and 50-km fiber links and 5 Gbps for 100-km fiber link. The proposed scheme for 20-km fiber link demonstrates the best transmission performance with a simple and cost-effective structure. By increasing the transmission distance to 50-km, the EVM performance only increase about 0.9% which still can support 64-QAM modulation format. For 100-km fiber transmission, the proposed scheme still can achieve the data rate of 5 Gbps by the simple method to mitigate the severe RF fading effect.

4. Conclusions

We proposed and experimentally demonstrated a 24-GHz RoF transmission system for supporting different transmission distances based on a directly modulated transmitter. Since the DFB laser performs as a light source and a signal modulator concurrently, it can simplify the RAN transmitter design with a better cost-efficiency. The characteristics of the DFB laser are measured to ensure that it is operated in the best condition to carry QAM signals. The experimental results exhibit that the direct modulation scheme can achieve the EVM performance of 5.98% /6.87% /10.8% with the data rate of 6/6/5 Gbps for 20-/50-/100-km fiber links, respectively. Thus, the proposed MMW-RoF scheme with a simple design can support a Gbps-class data rate for different transmission distances in the RAN architecture.

References

[1] G. K. Chang and Y. W. Chen, “Key fiber wireless integrated radio access technologies for 5G and beyond,” in *Proc. Opto-Electron. Commun. Conf.*, 2019, pp. 1–3.

[2] J. Zhang, J. Yu, and N. Chi, “Transmission and full-band coherent detection of polarization-multiplexed all-optical Nyquist signals generated by Sync-shaped Nyquist pulses,” *Sci. Rep.*, vol. 5, 2015, Art. no. 13649.

[3] Z. Jia, H. Chien, J. Zhang, Y. Cai, and J. Yu, “Performance comparison of dual-carrier 400G with 8/16/32-QAM modulation formats,” *IEEE Photon. Technol. Lett.*, vol. 27, no. 13, pp. 1414–1417, Jul. 2015.

[4] M. H. M. Shamim *et al.*, “Investigation of self-injection locked visible laser diodes for high bit-rate visible light communication,” *IEEE Photon. J.*, vol. 10, no. 4, Aug. 2018, Art. no. 7905611.

[5] C. W. Hsu, C. W. Chow, and C. H. Yeh, “Cost-effective direct-detection all-optical OOK-OFDM system with analysis of modulator bandwidth and driving power,” *IEEE Photon. J.*, vol. 7, no. 4, Aug. 2015, Art. no. 7902607.

[6] R. K. Shiu *et al.*, “Tunable microwave photonic filter for millimeter-wave mobile fronthaul systems,” in *Proc. IEEE Photon. Conf.*, 2018, pp. 1–2.

[7] S. Donati and V. Annovazzi-Lodi, “From order to chaos and back: Recent advances in optical cryptography of transmitted data,” in *Proc. Int. Conf. Adv. Optoelectron. Lasers*, 2013, pp. 1–6.

[8] C.-H. Yeh and C.-W. Chow, “Using single side-band modulation for colorless OFDM-WDM access network to alleviate Rayleigh backscattering effects,” *Opt. Express*, vol. 24, no. 10, pp. 10898–10903, 2016.

[9] G. K. Chang and P.C. Peng, “Grand challenges of fiber wireless convergence for 5G mobile data communications [Invited],” in *Proc. Opto-Electron. Commun. Conf.*, 2018, pp. 1–2.

[10] C. W. Chow, J. Y. Sung, and C. H. Yeh, “A convergent wireline and wireless time-and-wavelength-division-multiplexed passive optical network,” *IEEE Photon. J.*, vol. 7, no. 3, Jun. 2015, Art. no. 7902107.

[11] C. W. Chow, S. P. Huang, L. G. Yang, and C. H. Yeh, “Extended-reach access network with downstream radio-over-fiber (ROF) signal and upstream NRZ signal using orthogonal-WDM,” *Opt. Express*, vol. 20, no. 16, pp. 16757–16762, 2012.

[12] X. Li, J. Yu, J. Xiao, N. Chi, and Y. Xu, “W-band PDM-QPSK vector signal generation by MZM-based photonic frequency octupling and precoding,” *IEEE Photon. J.*, vol. 7, no. 4, Aug. 2015. Art.no. 7101906.

[13] A. S. Gowda, A. R. Dhaini, L. G. Kazovsky, H. Yang, S. T. Abraha, and A. Ng’oma, “Towards green optical/wireless in-building networks: Radio-over-fiber,” *J. Lightw. Technol.*, vol. 32, no. 20, pp. 3545–3556, Oct. 2014.

[14] C. T. Tsai, C. H. Lin, C. T. Lin, Y. C. Chi, and G. R. Lin, “60-GHz millimeter-wave over fiber with directly modulated dual-mode laser diode,” *Sci. Rep.*, vol. 6, pp. 27919-1–27919-12, 2016.

[15] G. Keiser, *Optical Fiber Communication*. New York, NY, USA: McGrawHill, 2013.

[16] L. Zhao *et al.*, “Polar coded OFDM signal transmission at the W-band in millimeter-wave system,” *IEEE Photon. J.*, vol. 11, no. 6, Dec. 2019, Art. no. 7907206.

[17] X. Li, J. Zhang, J. Xiao, Z. Zhang, Y. Xu, and J. Yu, “W-band 8QAM vector signal generation by MZM-based photonic frequency octupling,” *IEEE Photon. Technol. Lett.*, vol. 27, no. 12, pp. 1257–1260, Jun. 2015.

[18] C. Lim *et al.*, “Fiber-wireless networks and subsystem technologies,” *J. Lightw. Technol.*, vol. 28, no. 4, pp. 390–405, Feb. 2010.

[19] C.-T. Lin *et al.*, “Optical direct-detection OFDM signal generation for radio-overfiber link using frequency doubling scheme with carrier suppression,” *Opt. Express*, vol. 16, no. 9, pp. 6056–6063, 2008.

[20] K. Van Gasse *et al.*, “480Mbps/1 Gbps radio-over-fiber link based on a directly modulated III-V-on-silicon DFB laser,” in *Proc. IEEE Int. Topical Meeting Microw. Photon.*, 2016, pp. 328–331.

[21] J. V. Kerrebrouck *et al.*, “10 Gb/s radio-over-fiber at 28 GHz carrier frequency link based on 1550 nm VCSEL chirp enhanced intensity modulation after 2 km fiber,” in *Proc. Opt. Fiber Commun. Conf.*, 2018, pp. 1–3.

[22] J. Bohata, M. Komanec, J. Spáčil, Z. Ghassemlooy, S. Zvánovec, and R. Slavík, “24-26 GHz radio-over-fiber and free-space optics for fifth-generation systems,” *Opt. Lett.*, vol. 43, no. 5, pp. 1035–1038, 2018.

[23] P. C. Peng *et al.*, “Multiwavelength laser module based on distribute feedback laser diode for broadcast and communication systems,” *IEEE Photon. J.*, vol. 8, no. 4, Aug. 2016, Art. no. 1503208.

[24] X. Li, J. Xiao, and J. Yu, “Large-capacity long-distance wireless mm-wave signal delivery at W-band,” in *Proc. Int. Conf. Wireless Commun. Signal Process.*, 2015, pp. 1–6.

[25] Y.-W. Chen *et al.*, “Constructed MC-CDMA LR-PON with colorless laser diode and multicode interference cancellation DSP,” *J. Lightw. Technol.*, vol. 35, no. 13, pp. 2646–2653, Jul. 2017.

[26] R. Schmogrow *et al.*, “Error vector magnitude as a performance measure for advanced modulation formats,” *IEEE Photon. Technol. Lett.*, vol. 24, no. 1, pp. 61–63, Jan. 2012.

[27] R. A. Shafik, S. Rahman, and R. Islam, “On the extended relationships among EVM, BER and SNR as performance metrics,” in *Proc. Int. Conf. Elect. Comput. Engi.*, 2006, pp. 408–411.